Small scale simulations of outrunner blocks

Lars Engvik, Fabio V. De Blasio & Anders Elverhøi

Engvik, L.,De Blasio, F. V.& Elverhøi, A.: Small scale simulations of outrunner blocks. *Norwegian Journal of Geology*, Vol. 86, pp. 301-307. Trondheim 2006. ISSN 029-196X.

Submarine debris flows are often accompanied by isolated blocks located some distance beyond the rest of the failed mass. These so-called outrunner blocks have the ability to travel over long distances on very gentle slopes. Glide tracks of various depths are observed in some cases, while in others no traces of significant erosion can be detected, which indicates that outrunner blocks are able to travel completely separated from the bed. Similar phenomena occur in laboratory experiments, where chunks detach from the front of a small-scale debris flow and move out ahead of the rest of the flow. We present a two-dimensional, small-scale model of a rigid block subjected to gravity combined with the complete dynamical interaction with the surrounding liquid. Our simulations indicate that the block is able to hydroplane completely separated from the bed and attain long runout distances. The maximum velocity of the block is close correlated with the thickness of the block. For the simple shape assumed in our model we find that the densimetric Froude number is ≤0.8 . Depending on the geometrical shape of the block, size and the slope angle, we observe oscillatory motion, where the front of the block is lifted periodically and the rear part tends to scrape the bed. The pressure distribution around the block indicates that the block is likely to deform at the rear end as well as the front.

Lars Engvik, Sør Trøndelag University College, NO-7005 Trondheim, Norway; Fabio V. De Blasio and Anders Elverhøi, Department of Geosciences, University of Oslo, P.O. Box 1047 Blindern, NO-0316 Oslo, Norway, and International Centre for Geohazards, c/o Norwegian Geotechnical Institute, P.O. Box 3930 Ullevål Stadion, NO-0806 Oslo, Norway.

Introduction

Submarine debris-flow deposits are often accompanied by isolated blocks located some distance beyond the rest of the failed mass. These so-called outrunner blocks are able to travel over long distances even on very gentle slopes. Outrunner blocks have been reported from Kitimat in Canada (Prior et al. 1982), the Nigerian sea (Nissen et al. 1999), the Faroe margin (Kuijpers et al. 2001) and Finneidfjord in Norway (Longva et al. 2003; Ilstad et al. 2004).

In some cases like Finneidfjord, only tiny traces of significant erosion are visible, while in others like the Nigerian sea, glide tracks up to 10 meters deep and 250 meters wide have been reported, matching the size of the block itself. Blocks appear to be elongated in shape, with the major axis directed perpendicular to flow direction. Similar events are observed in laboratory experiments with subaqueous debris flows (Mohrig et al. 1998; Ilstad et al. 2004). A lubricating water layer is formed under the frontal part of the debris flow that increases its mobility and chunks of material are able to detach from the front and come to rest well separated from the rest of the debris flow deposits. The laboratory experiments provide a means to understand the formation and flow of outrunner blocks, as well as the frontal dynamics of subaqueous debris flows in general.

The recent work by Ilstad et al. (2004) deals with the blocks of Finneidfjord, and focuses on the comparison with experimentally created outrunner blocks and on the mechanics of block detachment. Understanding the generation and dynamics of outrunner blocks could shed light on the problem of the extraordinary mobility of subaqueous landslides. A more general review on the mobility of submarine debris flows is given in this special issue by De Blasio et al. (2006a). Recently, we have investigated a simple hydrodynamic model of a rigid block interacting with ambient water and subject to lubrication with the sea floor (De Blasio et al 2006b). With appropriate values of lift forces and water lubrication, the block was able to reach long runouts, in agreement with data. Furthermore, oscillating motion of the block arose naturally from the numerical solution, which could explain the creation of periodic grooves in the glide tracks seen Nigerian and Faroe blocks. However, a complete understanding of the dynamics of the outrunner block cannot be achieved without detailed knowledge of the water flow. An investigation of the dynamics of outrunner blocks has been performed by Harbitz et al (2003), who provided an analytical model for the water flow under the block based on lubrication theory, and is applied to determine the dynamics of outrunner blocks. However, it is not possible to determine fluid flow completely analytically. In this work we will calculate the torque as well as the forces on the outrunner block explicitly by direct numerical simulation of the complete fluid flow around the block. This is a so-called fluid-structure calculation that has been studied in great detail for isolated objects. To our knowledge, this is the first time this kind of calculation

is applied to investigate the movement of outrunner blocks. In this work we will study the small scale problem, where the relatively complex fluid flow can be determined accurately.

The aim of the work is to characterize the motion of an outrunner block, in terms of periodicity and maximum speed, depending on its size and on the slope angle. We perform calculations for various Reynolds numbers, or equivalently various sizes of the block as well as different slope angles.

For simplicity we restrict ourselves only to a simple shaped body. To investigate the sensitivity to the shape of the body, we also vary the relative length of the block.

The hydroplaning block model

The dynamics of a block sliding on the sea bed is determined by the gravity force, the block interaction with the fluid, and resistance exerted on the block by the sea bottom. In contrast to gravity, whose magnitude is constant, the other forces depend on the velocity, mass, shape, and orientation of the block. Additionally, the interaction with the sea floor is complicated by geometrical irregularities, bed composition and excess pore pressure generation. The block is thus subjected to a complicated system of forces and torques.

In producing a tractable model, we have simplified the geometry and restricted the number of degrees of freedom allowed during block movement. We assume a rigid plate of constant width W, thickness H and length L with smooth surfaces and rounded edges. The motion of the fluid as well as the block is restricted to two dimensions with directions down slope and normal bed. The block is completely separated from the bed, surrounded by fluid and hence, does not interact directly with the bed via friction or normal forces. The dynamics of the body is examined by direct numerical simulations, where the coupled system of equations describing motion for the body and the fluid is solved numerically with the finite element package FEMLAB®. The hydroplaning block model is characterized by seven parameters: The thickness H and length L, the densities of the fluid ρ_w and plate ρ, the dynamic viscosity of the fluid η, the slope angle θ and the gravitational acceleration g.

The outrunner block becomes separated from the bed when it cannot displace the ambient fluid fast enough. A stagnation pressure in the front which is proportional to $\rho_w u_c^2$, where u_c is the centre of mass velocity of the block, determines a separation of the block from the bed (Mohrig et al. 1998). When the block is completely separated from the bed, and maintains an horizontal position, the water layer must support the submerged load per unit area from the block $(\rho-\rho_w)gH$. The square root of the ratio of these expressions defines the densimetric Froude number

$$F^* = \frac{u_c}{\sqrt{\frac{\rho-\rho_w}{\rho_w} gH}},$$

Note that this definition is slightly different from the one used by e.g., Mohrig et al. (1998) and Ilstad et al. (2004) where the Froude number depends on the slope angle θ. However, we find the above definition more convenient in the investigation of the hydroplaning phase where the orientation of the block may change with time. We define the characteristic velocity for the object by

$$U = \sqrt{\frac{\rho-\rho_w}{\rho_w} gH}.$$

The characteristic time is then

$$\tau = \frac{H}{U}.$$

We also introduce the characteristic Reynolds number by

$$Re = \frac{\rho_w U H}{\eta} = \frac{\sqrt{g\rho_w(\rho-\rho_w)H^3}}{\eta}.$$

The fluid flow is described by the Navier-Stokes equation

$$\rho_w\left[\frac{\partial \boldsymbol{u}}{\partial t}\right] + ((\boldsymbol{u}-\boldsymbol{w})\cdot\nabla)\boldsymbol{u} - \nabla\cdot\eta\left(\nabla\boldsymbol{u} + (\nabla\boldsymbol{u})^T\right) + \nabla p = \boldsymbol{0} \qquad (1)$$

and continuity

$$\rho_w\left[\frac{\partial \boldsymbol{u}}{\partial t}\right] + ((\boldsymbol{u}-\boldsymbol{w})\cdot\nabla)\boldsymbol{u} - \nabla\cdot\eta\left(\nabla\boldsymbol{u} + (\nabla\boldsymbol{u})^T\right) + \nabla p = \boldsymbol{0} \qquad (2)$$

where $\boldsymbol{u}=(u_x,u_y)$and w=(w_x,w_y) are the fluid and mesh velocities, respectively, and p is the pressure. The mesh velocity accounts for the motion of the block and is determined within the Arbitrary Lagrangian Eulerian technique discussed below.

The moving block imposes boundary velocities on the fluid. The fluid motion generates reaction forces on the block that alter its motion. Both the linear and rotational dynamics of the block are taken into account by

$$m\frac{d\boldsymbol{u}_c}{dt} = \boldsymbol{G}_B + \boldsymbol{F}, \quad I\frac{d\omega}{dt} = \Gamma, \qquad (3)$$

where $\boldsymbol{u}_c=(u_{cx},u_{cy})$is the centre of mass velocity, ω is its angular velocity, m is the mass of the block, I is its moment of inertia. Furthermore, $\boldsymbol{G}_B$ is the combined gravitational and buoyant force, $\boldsymbol{F}$ is the net fluid force and Γ is the torque, to which the block is subjected. These values are determined by the fluid flow using the Navier-Stokes model, together with the stress tensor

$$\sigma = -p\mathbf{I} + \eta\left(\nabla\boldsymbol{u} + (\nabla\boldsymbol{u})^T\right)$$

where $\boldsymbol{I}$ is a unit diagonal matrix. The fluid force on the block is given by integrating the normal component of the stress tensor over the surface of the block S:

$$\boldsymbol{F} = \int_S dS\boldsymbol{n}\cdot\sigma\,, \tag{4}$$

where $\boldsymbol{n}$ is the normal vector of the block surface.

Furthermore, the torque of the block is given by the integral

$$\Gamma = \int_S \boldsymbol{r}\times(\boldsymbol{n}\cdot\sigma)dS\,, \tag{5}$$

where $\boldsymbol{r}=(x-x_c,y-y_c)$ is the position on the surface relative to the centre of mass.

To track the block motion, we use the Arbitrary Lagrangian Eulerian technique as described in Donea & Huerta (2003), Donea et al. (2003) and FEMLAB User's manual, 3.1 edition (2004). We apply a computational domain that follows the centre of mass of the block along the bed as shown in figure 2. The position of the mesh and the mesh velocity are represented by field variables, and the Laplace equation is used to determine the mesh velocity

$$\nabla^2\boldsymbol{w} = 0\,. \tag{6}$$

This equation is solved with appropriate boundary conditions determined by the motion of the plate. The velocity at the boundary of the plate is given by

$$\boldsymbol{u}_b = \boldsymbol{u}_c - (\boldsymbol{r} - \boldsymbol{r}_c)\times\boldsymbol{\omega}\,,$$

where $\boldsymbol{r}$ is the position on the surface of the block and $\boldsymbol{r}_c$ is the centre of mass position. The fluid flow and mesh velocities are constrained by boundary conditions:
$\boldsymbol{u}=\boldsymbol{0}$ and $\boldsymbol{w}=\boldsymbol{u}_c$ on boundaries A
$\boldsymbol{u}=\boldsymbol{u}_b$ and $\boldsymbol{w}=\boldsymbol{u}_b$ on boundary B
$p=0$ and $\boldsymbol{w}=\boldsymbol{u}_c$ on boundary C.

Thus the fluid is at rest when it enters the computational domain in the front and it leaves the computational domain at boundary C with zero pressure. The equations (1-4) are implemented numerically using the so-called Weak form application mode provided by FEMLAB, with the boundary conditions given above. Note that the position (x_c,y_c) and orientation of the block is determined by integrating the center of mass velocity and angular velocity, respectively, with respect to time. The orientation of the block is denoted θ_c

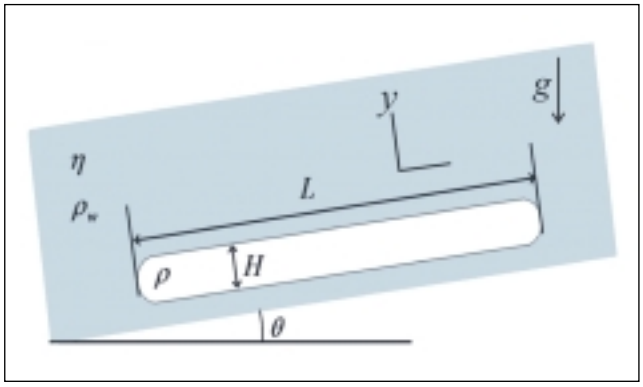

Fig 1: The important parameters entering the hydroplaning block model. See text for explanation.

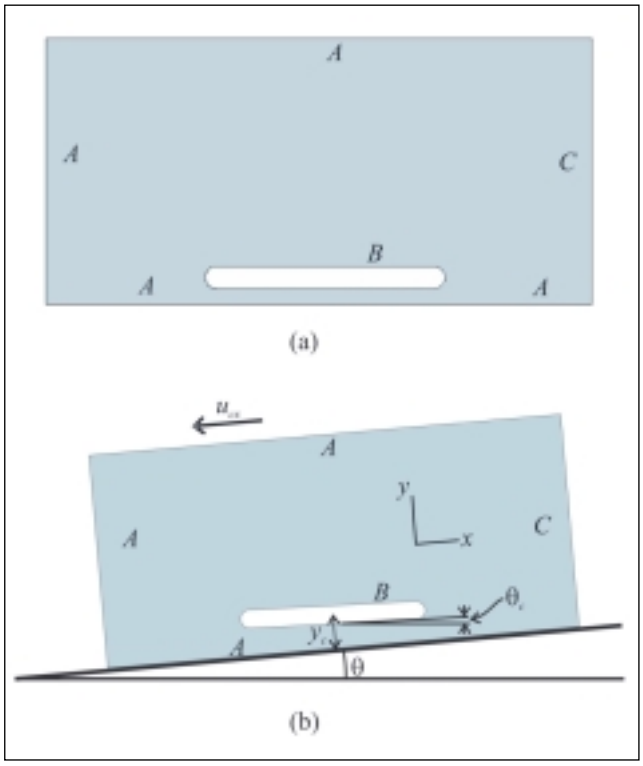

Fig 2: The computational domain applied in the calculation is shown in (a). For the boundaries A, B and C referred to in the text, different boundary conditions are applied. The physical domain for a typical slope angle at a given time is shown in (b). The physical domain is moving along the slope according to the center of mass velocity and the motion of boundaries B is determined by the angular velocity of the block as well as its center of mass velocity. The position of the center of mass normal to the bed is denoted y_c, while the orientation of the block is θ_c.

Results

We apply the numerical method to study the dynamics of the block along an inclined bed. The aim is to see how the Reynolds number, geometrical shape and the slope affect the dynamics. The block is initially at rest and oriented parallel to the bed, i.e., $\theta_c=\theta$, with the centre of mass $y_c=1.25H$ above the bed. Time dependent calculations have been performed up to more than 250τ, which is sufficient for the block to reach the terminal velocity and to develop several periods of oscillatory motion. In table 1 we show two sets of physical properties and dimensions, consistent with a characte-

ristic Reynolds number Re=686. In the calculations presented below the characteristic Reynolds number is varied by an order of magnitude from 69 to 686.

Table 1.

H [m]	L [m]	ρ [kg/m^3]	η [Pa s]	τ [s]	U [m/s]
0.02	0.2	1600	0.01	0.058	0.34
0.0043	0.043	1600	0.001	0.027	0.16

Table 1: Two sets of physical properties and dimensions consistent the calculations with a characteristic Reynolds number of Re=686 The first data set is consistent with the experimental data sets studied by Mohrig et al. (1998) and Ilstad et al. (2004). The second data set is equivalent to the outrunner block moving in pure water.

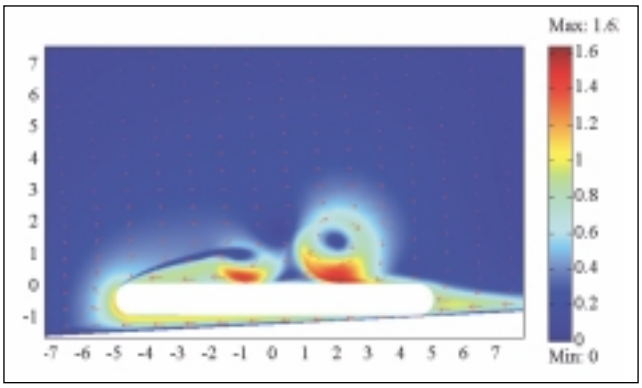

Fig 3: The magnitude of the velocity field around a hydroplaning block at a given time 244τ after release. The characteristic Reynolds number is Re=686 and the slope angle is θ=3°.

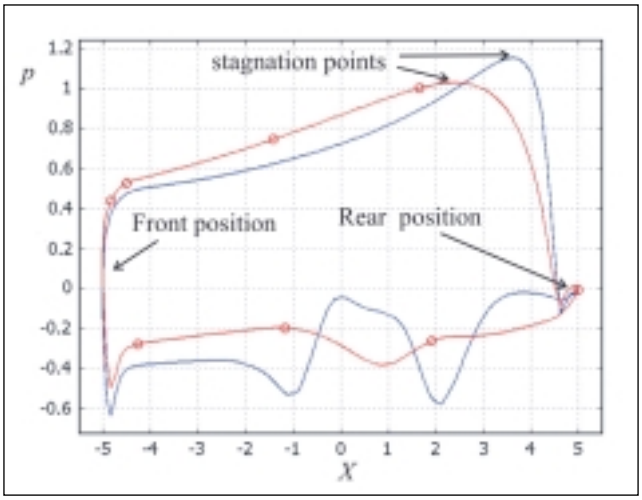

Fig 4: The pressure distribution around the block plotted as a function of the longitudinal position X on the block. The red curve with circles shows the results at 156τ while the blue solid curve is the result at t=244τ. The upper parts of the respective curves correspond to the pressure under the block, and the lower parts of the curves represent the pressure at the top of the block.

Figure 3 shows the magnitude of the velocity field around the block after its terminal velocity of $u \approx 0.8U$ has been reached. At this velocity the front of the block is lifted to an almost horizontally position resulting in an increased drag that balances the gravitation. A flow separation is seen on top of the block that brings about instabilities in the fluid flow that induce oscillations on the motion of the block.

The main contribution to the force and torque originates from the pressure distribution around the block. In figure 4 we show the pressure distribution as a function of the longitudinal position relative to the centre of mass position $X=(x-x_c)\cos(\theta_c-\theta)-(y-y_c)\sin(\theta_c-\theta)$ at two different times.

At t=156τ (red curve) the front of the block is relatively close to the bed and the block is oriented parallel to the bed. At t=244τ (blue curve) the front of the block is lifted up. Note that at the very front of the block the pressure is close to zero. This reflects the fact that most of the fluid is transported over the block and that there is a relatively high vertical fluid velocity at the front. The pressure increases along the surface under the block and reaches its maximum at the stagnation point. Note that there is a pressure excess under the block due to the stagnation of the fluid. We find that the stagnation point is situated significantly behind the centre of mass position. In fact for a block of constant thickness we find that the stagnation point is relatively close to the rear end, resulting in a very steep pressure drop behind the stagnation point. A local minimum of the pressure is found close to the point of minimum separation between the block and the bed.

There is a sharp drop in the pressure from the front of the block to the top where the global minimum pressure usually occurs. However, the pressure on top of the block is characterized by large variations with space and time mainly due to the flow separation which depends strongly on the orientation of the block. The strongest variations are found when the front of the block is lifted up.

Our results clearly indicate that there are large pressure gradients at the front of the block as well as at the rear end. If we take into account the weight per unit area of the block, we find that the block is exposed to an upward bending stress at the front while at the rear part of the block is pulled down by gravity as the pressure difference vanishes. This is consistent with observations in the small scale experiments of Mohrig et al. (1998) where large deformation is observed in the front as the sediment is lifted up and the rear part is elongated and depressed.

It is instructive to study the motion of the block as a function of time. In figure 5 the orientation and ave-

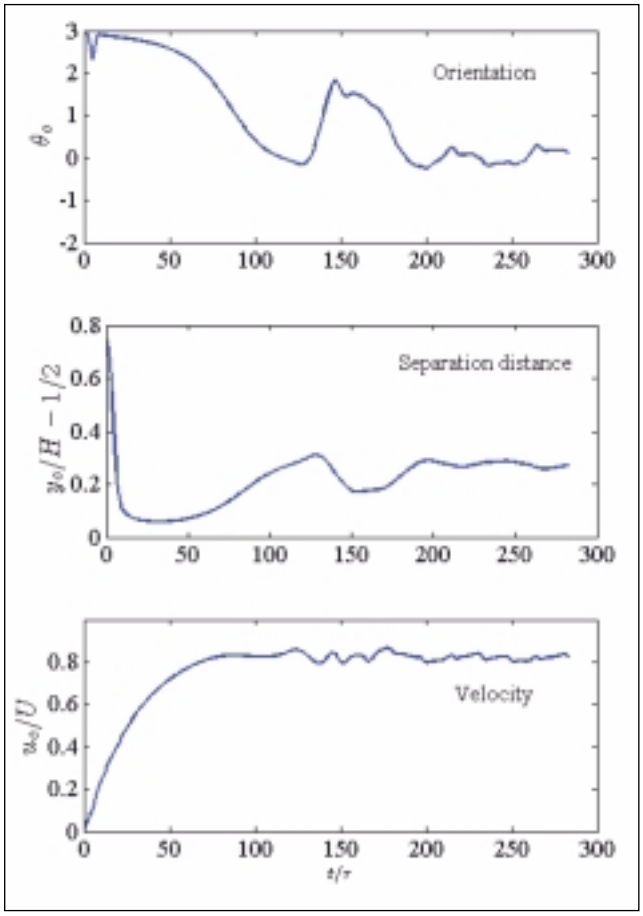

Fig 5: The orientation of the block , the average distance between the block and the bed, and the velocity of the block as functions of time. Note that denotes the position of the center of mass normal the bed The characteristic Reynolds number is 686 and the slope angle is 3°.

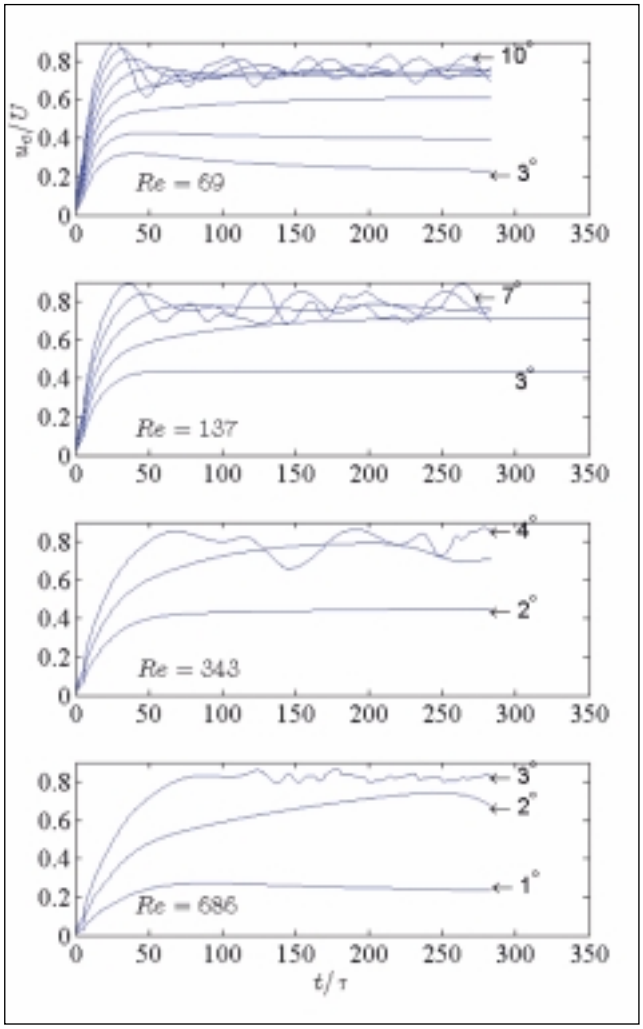

Fig 6: The speed of the block as a function of time. The characteristic Reynolds numbers and slope angles are indicated.

rage separation distance between the block and the bed together with the velocity is shown.

After the block is released, it quickly loses height above the bed and accelerates continuously along the bed. As the block begins to fall, water quickly escapes at the rear end. Due to the immediate down slope acceleration of the block, there is a significantly higher pressure under the front of the block. Thus the block immediately starts to orientate itself more horizontally as seen by the immediate drop in θ_c from 3° to 2.3°. This effect is similar to what is observed for freely falling objects, where a fluttering or tumbling motion has been reported (Belmonte et al. 1998; Field et al. 1997). However, as the block gets close to the bed, the water is obstructed and the pressure increases rapidly, preventing the rear end of the block to touch the bed. The block recaptures its original orientation very close to the bed approximately at time 10τ. The speed of the block is still small but increasing. The motion of the block normal to the bed is found to be very slow compared to the motion parallel to the bed. The maximum speed normal to the bed is reflected in the rapid decrease in separation distance during the initial stage observed and is about $0.1U$.

The centre of mass distance to the bed starts to increase slowly again when the speed of the block has reached $0.5U$, i.e., the densimetric Froude number is 0.5. In the experiments of Mohrig et al. (1998), the sediment could separate from the bed if the densimetric Froude number exceeded 0.33.

As the block approaches the maximum speed, which is close to $0.8U_o$, the front of the block rises so that the block is orientated horizontally, while the rear part of the block remains close to the bed.

When the front of the block rises and the terminal velocity is reached, there is a flow separation at the top that generates an oscillatory motion of the block.

The orientation is generally highly correlated with the centre of mass height above the bed. This is because the rear end of the block is kept close to the bed, while the front separation varies significantly over time. However, in Fig. 5 small fluctuations in the orientation that do not have a counterpart in the centre of mass height, can be seen. These fluctuations, which occur only at the highest Reynolds numbers, reflect the variation of the separation distance between the rear end of the block and the bed, and also affect the speed of the block significantly.

We have investigated the motion of the block for different slope angles and Reynolds numbers. In figure 6 we plot the speed of the block for Reynolds numbers 69, 137, 343, and 686 on various slopes. At low Reynolds numbers the potential energy released by the falling block is efficiently consumed by the fluid, and the block attains a stationary streamlined motion for gentle slopes. At larger slope angles the front of the block lifts up to an almost horizontal orientation that increases the drag, and prevents the speed of the block to exceed $u \approx 0.8 U_c$.

It is useful to compare our results to the situation of a freely falling plate. An estimate of the terminal velocity of a rectangular plate with thickness H and area A_0 is given by the balance between the gravity $G=A_0H(\rho-\rho_w)$ and the drag force $F_D=C_D\rho U_t^2 A_0/2$, where C_D is the so-called drag coefficient. This gives the terminal velocity expressed in terms of the drag coefficient by

$$U_t = \sqrt{\frac{2(\rho-\rho_w)gH}{\rho_w C_D}} = \sqrt{\frac{2}{C_D}}U .$$

For the extreme case of a thin flat plate normal to the direction of motion, the drag coefficient approaches $C_D \approx 2$ and the teminal velocity simply becomes $U_t = U$. This is consistent with the results found in our simulations. Our results indicate that the maximum speed of the block is reached as the front of the block is lifted to a horizontal position. Thus the speed of a rigid flat plate is not likely to exceed U.

In our simulations we find that the motion of the block becomes non-stationary at steep slopes. The front oscillates markedly while the rear part of the block remains close to the bed. Our model does not take into account the possibility of bed erosion. However, we find that the amplitude of the oscillations increases with the slope angle and that the water layer under the rear part of the block is not maintained during these oscillations. Our simulations indicate that the block is likely to scrape the bed, periodically, and reminiscent of regularly dashed erosion marks observed for the Nigerian sea (Nissen et al. 1999) and the Faroe margin (Kuijpers et al. 2001).

To investigate the sensitivity to the length of the block we also have performed calculations for a block with half the length of the previous block., $H/L=5$. The results are presented in Figure 7.

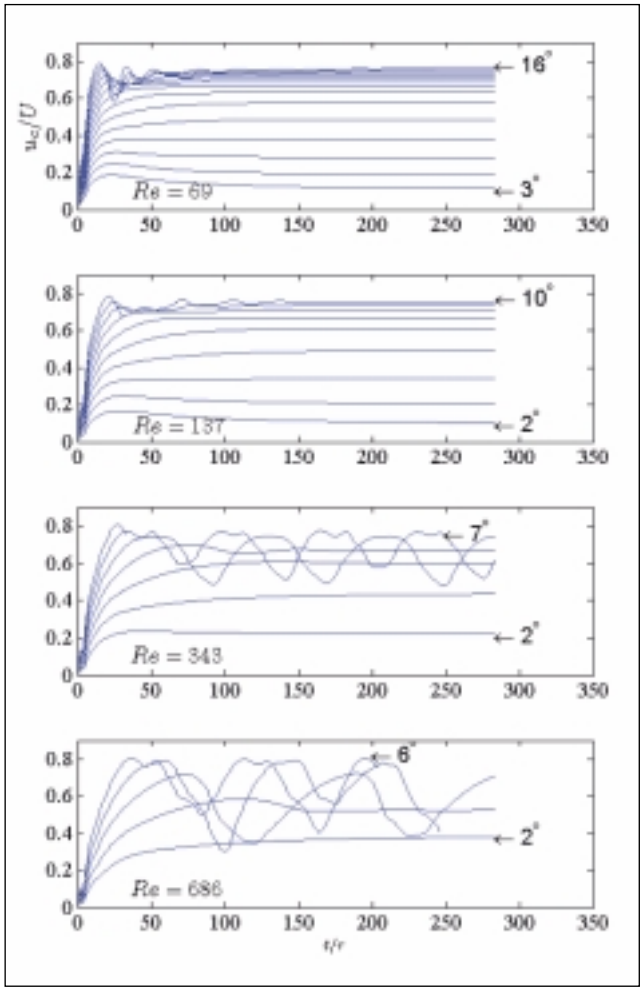

Fig 7: The speed of the short block with a height to length ratio . The characteristic Reynolds numbers and relevant slope angles are indicated. Results provided for each degree of bed slope.

Similar to our previous results with a longer block $H/L=10$, we find that the maximum speed of the block is close to $0.8U$. Note that the short block has less than half the weight of the long block we initially considered. It is more easily slowed down by the fluid forces, and therefore, the slope has to be relatively steep to attain a sufficient velocity to lift the front of the block.

At low Reynolds numbers we find that the initial oscillatory motion is quickly damped and the block attains a constant speed. The maximum speed that can be attained for steep slopes is slightly less than $0.8U$. At this velocity the block maintains in an almost horizontal position. At large Reynolds numbers $Re=343$ or 686 the friction from the fluid is less effective and persistent oscillations are seen for sufficiently steep slopes. Similar to the results for the long block, we find an oscillatory motion of the block at steep angles. The short block allowed for stronger variation in the orientation angle without touching the bed. For the largest Reynolds numbers we found periods of approximately 75τ.

Summary

To summarize, we have performed calculations of the motion of a rigid block with a constant thickness H in fluid along an inclined bed that takes into account the main dynamics of small scale outrunner blocks. This model takes into account the longitudinal and transverse motion of the liquid and block as well as the rotational dynamics of the block. We find that the maximum velocity of the block is not likely to exceed the characteristic velocity U which is proportional to $H^{3/2}$.

It is interesting to see that the mobility of the block is closely related to the characteristic Reynolds number. For a large Reynolds number ≥500 the outrunner block is able to maintain high velocities on gentle slopes, i.e., to ≤2 to 3˚.

The maximum velocity of the block is not strongly influenced by the slope angle or the length of the block, however it is constrained by the uplift of the front, which results in an increased drag.

Our simulations indicate periodical motion that becomes more apparent on steep slopes and is clearly affected by the length of the block. We generally find that the rear part of the block is kept very close to the bed, while the front part easily lifts up even at low angles. When the slope angle is large (about 4-10˚ depending on Reynolds numbers) we find large oscillations and we observe that the rear part of the block tends to hit the bed, an effect that also depends on the shape of the block. If the block is thicker at the front, it will touch the bed less frequently. It is also likely that the deformation of the block will have significant effects on the periodicity as well as on the maximum velocity. The results using the rigid block model indicate that an outrunner block is exposed to a dynamic pressure that is sufficient to cause deformation both at the rear part and in the front. This would clearly change the dynamics of the outrunner block and should be investigated.

Acknowledgements: This is International Centre for Geohazards contribution no. 95.

References

Belmonte, A., Eisenberg, H., & Moses, E. 1998: From Flutter to tumble: Inertial Drag and Froude Similarity in Falling Paper. *Physics Reviews and Letters* 81, 345-348.

De Blasio, F.V., Anders Elverhøi, A., Engvik, L. & Issler, D., J.P., Gauer, P., and Harbitz, C.B.. 2006a: Understanding the high mobility of subaqueous debris flows. *Norwegian Journal of Geology,* this issue.

De Blasio, F.V., Engvik, L. & Elverhøi, A. 2006b: The sliding of outrunner blocks from submarine landslides. *Geophysical Research Letters,* in press.

Donea, J. & Huerta, A. 2003: *Finite Element Methods for Flow Problems.* John Wiley & Sons, Chichester.

Donea, J. Huerta, A. Ponthot, J.-Ph. & Rodrígues-Ferran, A. 2004: "Arbitrary Langrangian-Eulerian Methods". In Stein, E. et al. (Eds.), Encyclopedia of Computational Mechanics. John Wiley & Sons.

Field, S.B., Klaus, M., Moore, M.G. & Nori, F. 1997: Chaotic dynamics of falling disks. *Nature* 388, 252-254.

Harbitz, C. B., Parker, G., Elverhøi, A., Marr, J., Mohrig, D. & Harff, P. 2003: Hydroplaning of subaqueous debris flows and glide blocks: Analytical solutions and discussion. *Journal of Geophysical Research* 108, B7, 2349, doi: 10.1029/2001JB001454.

Ilstad T., F. V. De Blasio, L. Engvik, A. Elverhøi, O. Longva, & J. Marr. 2004: On the frontal dynamics and morphology of submarine debris flows. *Marine Geology* 213, 481-497.

Kuijpers, A., Nielsen, T., Akhmetzhanov, A., de Haas, H., Kenyon, N. H. & van Weering, T. C. E. 2001: Late Quaternary slope instability on the Faroe margin: mass flow features and timing of events, *Geo-Marine Letters* 20, 149-159.

Longva, O., Janbu, N., Blikra, L.H. & Bøe, R. 2003: The 1996 Finneidfjord Slide: seafloor failure and slide dynamics. *In* J.Locat and J. Mienert (Eds.), *Submarine Mass Movements and their Consequences.* Proceedings First International Symposium. Kluwer Academic Publishers, Dordrecht, The Netherlands, 531-538.

Mahadevan, L., Ryu, W.S. & Samuel, A.D.T. 1999: Tumbling cards. *Physics of Fluids* 11, 1-3.

Mohrig, D., Whipple, K. X., Hondzo, M., Ellis, C. & Parker, G. 1998: Hydroplaning of subaqueous debris flows. *Geological Society of America Bulletin* 110, 387–394.

Nissen, S. E., Haskell, N. L., Steiner, C. T. & Coterill, K. L. 1999: Debris flow outrunner blocks, glide tracks, and pressure ridges identified on the Nigerian continental slope using 3D seismic coherency. *The Leading Edge, Society of Exploration Geophysicists* 18, 550-561.

Prior, D. B., Coleman, J. M. & Borhold, B. D. 1982: Results of a known sea floor instability event. *Geo-Marine Letters* 2, 117-122.